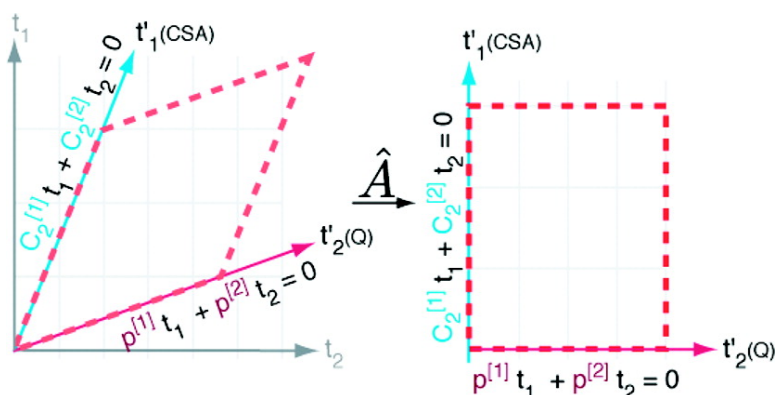


Separating Chemical Shift and Quadrupolar Anisotropies via Multiple-Quantum NMR Spectroscopy

Jason T. Ash, Nicole M. Trease, and Philip J. Grandinetti

J. Am. Chem. Soc., **2008**, 130 (33), 10858-10859 • DOI: 10.1021/ja802865x • Publication Date (Web): 25 July 2008

Downloaded from <http://pubs.acs.org> on February 8, 2009



More About This Article

Additional resources and features associated with this article are available within the HTML version:

- Supporting Information
- Access to high resolution figures
- Links to articles and content related to this article
- Copyright permission to reproduce figures and/or text from this article

[View the Full Text HTML](#)



ACS Publications
 High quality. High impact.

Separating Chemical Shift and Quadrupolar Anisotropies via Multiple-Quantum NMR Spectroscopy

Jason T. Ash, Nicole M. Trease, and Philip J. Grandinetti*

Department of Chemistry, The Ohio State University, 100 West 18th Avenue, Columbus, Ohio 43210-1173

Received April 25, 2008; E-mail: grandinetti.org/contact

The exploitation of chemical shift anisotropy (CSA) for probing structure and dynamics has a long history in magnetic resonance spectroscopy.¹ Phosphate-group² and base-pair orientations³ in nucleic acids, phospholipid headgroup interactions,⁴ and enantiomers of chiral molecules⁵ have all been investigated via CSA. Numerous applications also exist for the study of proteins, including probing hydrogen-bond formation and secondary structure,⁶ characterizing rapid internal motions,⁷ and analyzing the dynamics⁸ and conformations⁹ of protein backbones. The applications previously described involve the use of spin- $1/2$ nuclei such as ^1H , ^{13}C , ^{15}N , and ^{31}P . For these nuclei, the CSA can be measured in a variety of ways, including the use of cross-relaxation¹⁰ or liquid-crystalline solvents¹¹ in solution as well as the analysis of static spectra or magic-angle spinning (MAS) sidebands¹ in solids.

Nearly 70% of NMR-active nuclei have spin $I > 1/2$, and unfortunately, these nuclei exhibit large quadrupolar couplings that render most solution NMR methods for determining CSA ineffective. These couplings also complicate the analysis of solid-state experiments, as spectra must be fit for the principal components of both the chemical-shift and quadrupolar-coupling tensors as well as for their relative orientation.^{12–17} While techniques such as SAS¹⁸ and DACSY¹⁹ have shown significant improvement over traditional methods, they do not explicitly separate the CSA from the quadrupolar anisotropy, and thus, determination of the CSA still requires a large number of fit parameters. They also require rapid sample reorientation during the experiment, making them challenging to implement.

Wang et al.²⁰ proposed a solution for $I = 3/2$ nuclei in an experiment analogous to multiple-quantum magic-angle spinning (MQ-MAS)²¹ except that the rotor is oriented at a magic angle for rank-four interactions (70.12°) rather than the magic angle for rank-two interactions (54.74°). In this work, we expand upon this idea and demonstrate that with the use of appropriate affine transformations,²² the anisotropies of the chemical shift and the quadrupolar coupling can be correlated in orthogonal dimensions, making the technique applicable to all half-integer quadrupolar nuclei. We refer to this experiment as correlation of anisotropies separated through echo refocusing (COASTER).

The COASTER experiment is a triple-to-single-quantum correlation with a coherence transfer pathway of $p = 0 \rightarrow +3 \rightarrow -1$ while the sample is spun at 70.12° . This pathway refocuses the second-rank quadrupolar anisotropy and chemical shift at different times in the 2D experiment. As illustrated in Figure 1, the quadrupolar anisotropy refocuses along the line $C_2^{[1]}t_1 + C_2^{[2]}t_2 = 0$, where $C_2^{[n]}$ is the second-order rank-two coefficient of the quadrupolar coupling in the n th dimension. Similarly, the chemical shift refocuses along the line $p^{[1]}t_1 + p^{[2]}t_2 = 0$, where $p^{[n]}$ is the coherence order in the n th dimension. The appropriate affine transformation for separating these interactions decomposes into a shearing transformation along the ω_1 coordinate with ratio λ_1 followed by a scaling of ω_1 by a factor s_1 , after which ω_2 is sheared

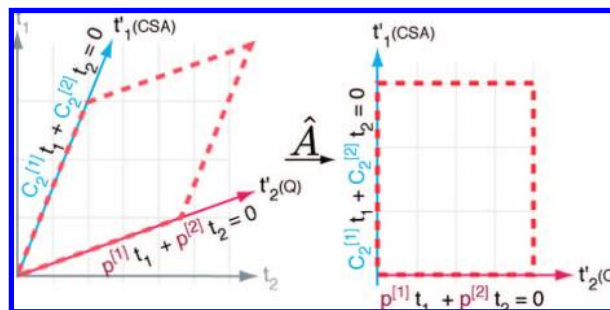


Figure 1. Quadrupolar-coupling and chemical shift anisotropies are separated into orthogonal time domains after the application of an affine transformation using the shearing and scaling parameters given in Table 1.

Table 1. Shearing Ratios (λ) and Scaling Factors (s) for the Two Dimensions in the COASTER Experiment

I	λ_1	s_1	λ_2	s_2
$3/2$	0	1	$1/3$	$3/4$
$5/2$	$15/8$	$8/23$	$23/9$	$9/32$
$7/2$	$12/5$	$5/17$	$17/3$	$3/20$
$9/2$	$21/8$	$8/29$	$29/3$	$3/32$

and scaled by λ_2 and s_2 , respectively (see Table 1 and the Supporting Information). Fourier transformation of the new time coordinates produces two frequency coordinates, which we label as ω_1' (CSA) and ω_2' (Q). The projection of the 2D COASTER spectrum onto the ω_2' (Q) axis yields a 1D spectrum that depends only on the principal components of the quadrupolar-coupling tensor and is independent of the principal components of the chemical-shift tensor and the relative orientation of the two tensors. Similarly, the projection onto the ω_1' (CSA) axis yields a 1D spectrum that contains only anisotropy from the chemical shift interaction and is independent of the second-rank anisotropic quadrupolar contribution to the transition frequency and the relative orientation of the two tensors. The isotropic chemical shift (δ_{cs}) is obtained from the isotropic shifts found in the ω_1' (CSA) and ω_2' (Q) projections. This separation of anisotropies permits an accurate determination of the principal components of both the quadrupolar-coupling and chemical-shift tensors. The relative orientation of the two tensors is obtained by analyzing the pattern within the 2D COASTER spectrum. When the two tensors are diagonal in the same coordinate system, the 2D spectrum contains a triangular pattern, except when the asymmetry parameters for both tensors are zero ($\eta_{\text{cs}} = \eta_{\text{q}} = 0$), where the pattern in the 2D spectrum becomes a line. The vertices of the triangle correspond to the principal components of each tensor and establish which components are aligned. When the two tensors are not diagonal in the same coordinate system, an elliptical pattern appears in the 2D spectrum.

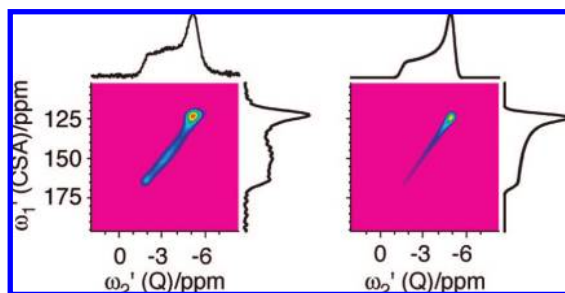


Figure 2. (left) ^{63}Cu COASTER spectrum of $\text{K}_3[\text{Cu}(\text{CN})_4]$ at 9.4 T referenced to 1 M KCN/0.1 M CuCN, along with (right) a simulation using the parameter values $C_q = 1.1$ MHz, $\delta_{cs} = -49$ ppm, $\zeta_{cs} = 30$ ppm, and $\eta_q = \eta_{cs} = 0$.

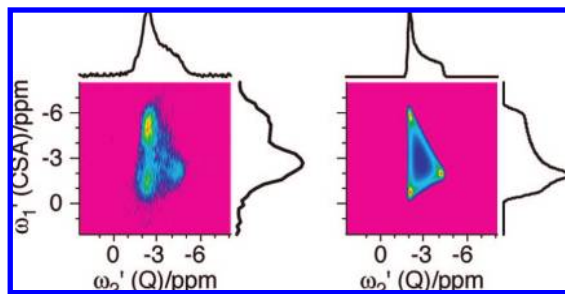


Figure 3. (left) ^{59}Co COASTER spectrum of $\text{K}_3[\text{Co}(\text{CN})_6]$ at 9.4 T referenced to 1 M $\text{K}_3[\text{Co}(\text{CN})_6]$, along with (right) a simulation using the parameter values $C_q = 6.2$ MHz, $\delta_{cs} = 14$ ppm, $\zeta_{cs} = -62$ ppm, $\eta_q = 1.0$, and $\eta_{cs} = 0.25$ and Euler angles $\alpha = 90^\circ$ and $\beta = \gamma = 0^\circ$.

If the chemical structure around a nucleus contains a symmetry axis, both the chemical shift and quadrupolar coupling often form axially symmetric tensors ($\eta_{cs} = \eta_q = 0$) that are aligned with the symmetry axis. For example, in $\text{K}_3[\text{Cu}(\text{CN})_4]$, a model $\text{Cu}(\text{CN})_4^{3-}$ structure that is popular for constructing supramolecular assemblies,²³ there is a C_3 axis along one of the Cu–CN bonds, and the largest principal components of both the chemical shift and quadrupolar coupling for ^{63}Cu are aligned with this axis.¹³ As shown in Figure 2, the ^{63}Cu COASTER projections confirm that both tensors are symmetric, and the narrow ridge in the 2D spectrum indicates that the tensors are diagonal in the same axis system.

Quadrupolar couplings generally depend only on the electronic ground state, whereas the chemical shift also depends on excited electronic states. For example, in an analogous cobalt complex, $\text{K}_3[\text{Co}(\text{CN})_6]$, there is a correlation between the ^{59}Co CSA and the ratio of the quadrupolar coupling constant, C_q , to the d–d transition energy.¹⁴ Thus, while the ^{59}Co quadrupolar coupling is asymmetric ($\eta_q = 1$),¹⁵ the CSA shows only a modest deviation from cylindrical symmetry ($\eta_{cs} = 0.25$). These differences in η_q and η_{cs} are observed in the 1D projections of the ^{59}Co 2D COASTER spectrum in Figure 3, which also shows a triangular pattern in the 2D spectrum, indicating that the tensors are still diagonal in the same axis system with the coincident components evident from the vertices of the triangle.

In Figure 4, we show the ^{87}Rb COASTER spectrum of RbCrO_4 , where the appearance of an elliptical pattern indicates that the tensors are not diagonal in the same coordinate system. The simulation indicates that $\beta = 70^\circ$, in agreement with previous measurements.¹⁶ Components of the chemical-shift tensor generally align with the crystal axes for many Rb and Cs salts.¹⁶ Thus, accurate measurement of the relative orientation allows one to determine the orientation of the quadrupolar-coupling tensor in the molecular frame without the need for ab initio calculations. Similar measurements could also be useful in carbonyl-containing systems

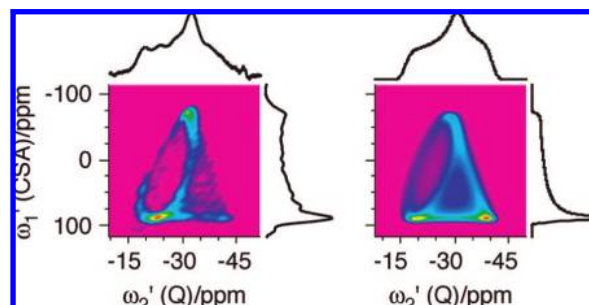


Figure 4. (left) ^{87}Rb COASTER spectrum of RbCrO_4 at 9.4 T referenced to 1 M RbNO_3 , along with (right) a simulation using the parameter values $C_q = 3.5$ MHz, $\eta_q = 0.36$, $\delta_{cs} = -9$ ppm, $\zeta_{cs} = -110$ ppm, $\eta_{cs} = 0$, $\alpha = \gamma = 0^\circ$, and $\beta = 70^\circ$.

such as proteins, where the ^{17}O quadrupolar-coupling tensor is always oriented along the carbonyl bond while substituent effects cause the chemical-shift tensor to rotate away from the bond.¹⁷

Since COASTER is performed at a fixed rotor axis, it can be implemented with minor modifications to most standard MAS probes. It should be noted that COASTER may be more appropriate for dilute or low- γ nuclei, where the off-magic-angle spinning will not reintroduce strong dipolar couplings that could complicate interpretation. Finally, although COASTER will not resolve overlapping sites, it is possible to extend the ideas presented here into a 3D experiment for increased resolution.

Acknowledgment. This material is based upon work supported in part by the National Science Foundation under Grant CHE0616881.

Supporting Information Available: Transition frequencies, data processing, and additional simulated examples. This material is available free of charge via the Internet at <http://pubs.acs.org>.

References

- (1) Herzfeld, J.; Berger, A. E. *J. Chem. Phys.* **1980**, *73*, 6021–6030.
- (2) Wu, Z. G.; Delaglio, F.; Tjandra, N.; Zhurkin, V. B.; Bax, A. *J. Biomol. NMR* **2003**, *26*, 297–315.
- (3) Gregory, D. M.; Mehta, M. A.; Shiels, J. C.; Drobny, G. P. *J. Chem. Phys.* **1997**, *107*, 28–42.
- (4) Pinheiro, T.; Watts, A. *Biochemistry* **1994**, *33*, 2451–2458.
- (5) Meddour, A.; Berdague, P.; Hedli, A.; Courtieu, J.; Lesot, P. *J. Am. Chem. Soc.* **1997**, *119*, 4502–4508.
- (6) Wu, C. H.; Ramamoorthy, A.; Gierasch, L. M.; Opella, S. J. *J. Am. Chem. Soc.* **1995**, *117*, 6148–6149.
- (7) Tjandra, N.; Bax, A. *J. Am. Chem. Soc.* **1997**, *119*, 8076–8082.
- (8) Fischer, M.; Zeng, L.; Pang, Y.; Hu, W. D.; Majumdar, A.; Zuiderweg, E. *J. Am. Chem. Soc.* **1997**, *119*, 12629–12642.
- (9) Heller, J.; Laws, D. D.; Tomaselli, M.; King, D. S.; Wemmer, D. E.; Pines, A.; Havlin, R. H.; Oldfield, E. *J. Am. Chem. Soc.* **1997**, *119*, 7827–7831.
- (10) Pervushin, K.; Riek, R.; Wider, G.; Wüthrich, K. *Proc. Natl. Acad. Sci. U.S.A.* **1997**, *94*, 12366–12371.
- (11) Rowell, J. C.; Phillips, W. D.; Melby, L. R.; Panar, M. *J. Chem. Phys.* **1965**, *43*, 3442–3448.
- (12) Cheng, J. T.; Edwards, J. C.; Ellis, P. D. *J. Phys. Chem.* **1990**, *94*, 553–561.
- (13) Kroeker, S.; Wasylishen, R. E. *Can. J. Chem.* **1999**, *77*, 1962–1972.
- (14) Chan, J.; Au-Yeung, S. *Annu. Rep. NMR Spectrosc.* **2000**, *41*, 1–54.
- (15) Nielsen, U. G.; Jakobsen, H. J.; Skibsted, J. *Solid State Nucl. Magn. Reson.* **2001**, *20*, 23–34.
- (16) Vosegaard, T.; Byriel, I. P.; Jakobsen, H. J. *J. Phys. Chem. B* **1997**, *101*, 8955–8958.
- (17) Wu, G.; Yamada, K.; Dong, S.; Grondey, H. *J. Am. Chem. Soc.* **2000**, *122*, 4215–4216.
- (18) Shore, J. S.; Wang, S. H.; Taylor, R. E.; Bell, A. T.; Pines, A. *J. Chem. Phys.* **1996**, *105*, 9412–9420.
- (19) Medek, A.; Sachleben, J. R.; Beverwyk, P.; Frydman, L. *J. Chem. Phys.* **1996**, *104*, 5374–5383.
- (20) Wang, S. H.; Xu, Z.; Baltisberger, J. H.; Bull, L. M.; Stebbins, J. F.; Pines, A. *Solid State Nucl. Magn. Reson.* **1997**, *8*, 1–16.
- (21) Frydman, L.; Harwood, J. S. *J. Am. Chem. Soc.* **1995**, *117*, 5367–5368.
- (22) Zwillinger, D. *CRC Standard Mathematical Tables and Formulae*; CRC Press: Boca Raton, FL, 1995; pp 265–266.
- (23) Ibrahim, A. *J. Organomet. Chem.* **1998**, *556*, 1–9.

JA802865X